

Direct Observations of Runaways following Disruptions in JET

R. D. Gill, B. Alper, A. W. Edwards, L. C. Ingesson, M. F. Johnson and D. J Ward¹

JET Joint Undertaking, Abingdon, Oxon., OX14 3EA, UK

¹*EURATOM/UKAEA Fusion Association, Culham Science Centre, Abingdon, Oxon., UK*

Introduction. Runaways generated during disruptions in tokamaks can have damaging consequences in large machines because of the high power generated by the localised deposition of the runaways on the vessel walls. Despite the maturity of this problem, little information is available about the details of the runaway beam. In most tokamaks the presence of the runaways only becomes apparent as they hit the vessel walls. However there are some measurements of the synchrotron¹⁾ and bremsstrahlung²⁾ radiation from the runaways in flight. Here we will report on new information obtained from observations on X-ray and bremsstrahlung emission from the runaways.

The disruptions. Loss of plasma thermal energy in disruptions occurs in two stages both

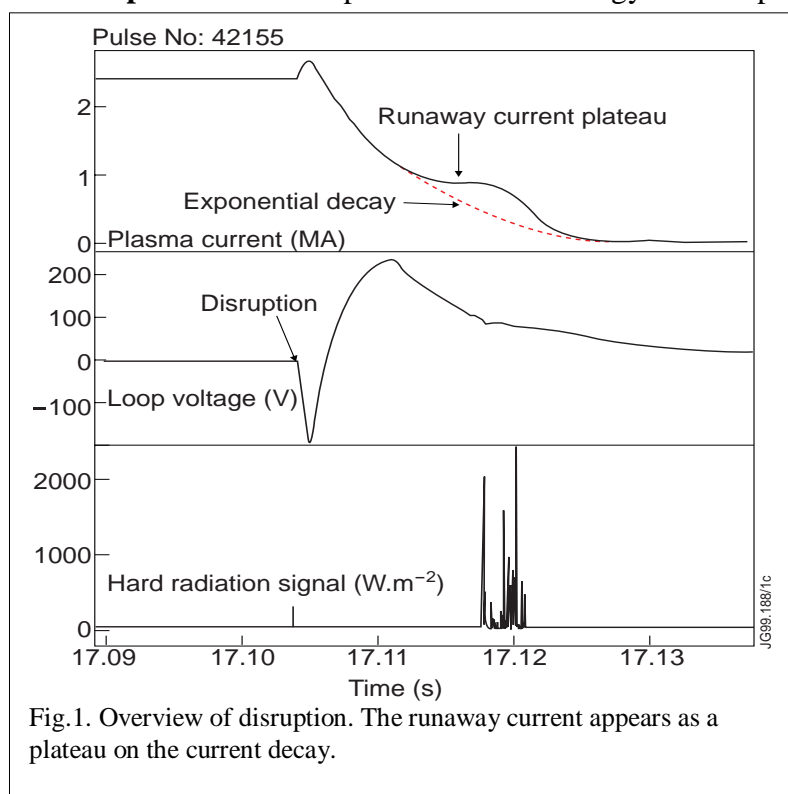


Fig. 1. Overview of disruption. The runaway current appears as a plateau on the current decay.

before and at the negative voltage spike. This produces a very large drop in electron temperature leading to electric fields within the plasma which are sufficient to produce substantial runaway currents. Although these currents sometimes persisted for seconds in earlier JET operation, in divertor plasmas short runaway tails only are seen, probably because of the reduced vertical stability, leading to rapid up or down movement of the current column. In addition, the loss of plasma pressure reduces the vertical field required for radial stability, but, as this field cannot be changed

on the required time-scale, the current column moves rapidly inwards. Departures from the initial exponential decay of the plasma current are caused by the generation of the runaways and are used to estimate their magnitude. These features may be seen for a JET discharge in Fig. 1 in which 0.6MA of runaways were generated.

The diagnostics. Observations have been made either with a set of compact X-ray cameras within the torus or with radiation protected cameras which view the plasma through opposite

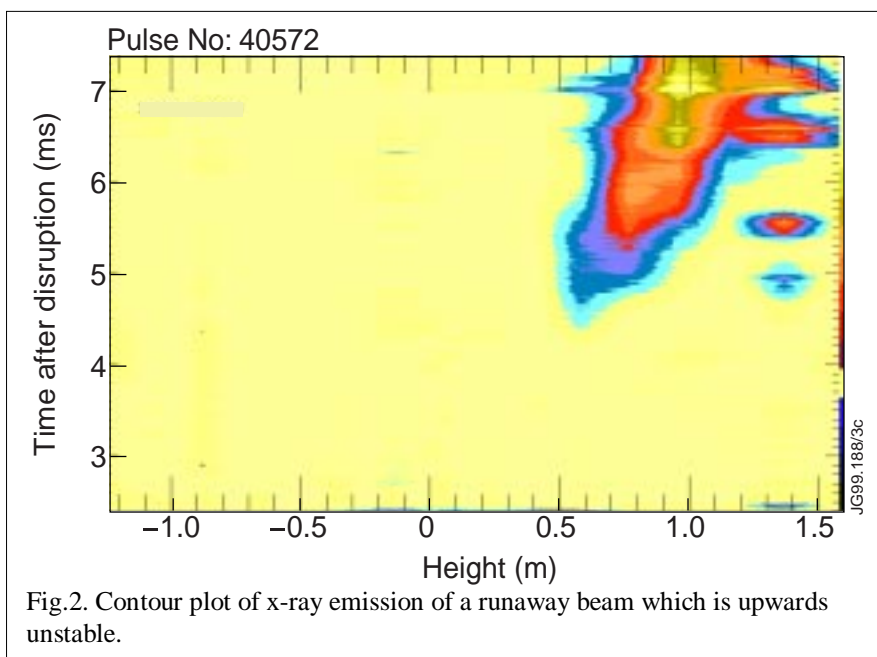
horizontal ports. The in-torus detectors are also sensitive to high energy γ -rays which can penetrate their cases. The detectors in the radiation protected cameras are sensitive to X-rays and γ -rays originating along their direct lines of sight only. In addition, each line of sight has a detector shielded from X-rays and sensitive only to γ -rays. Data is collected at high time resolution and good synchronisation by the CATS data acquisition system.

Bremsstrahlung. The runaways produce γ radiation in collisions with the residual atoms and ions which remain following the disruption. This radiation is concentrated by relativistic effects into a narrow forward cone with half angle $1/\gamma$. However, the radiation which reaches the detectors on the vessel walls will be spread over a considerable area both because of the motion of the runaways over their flux surface and because of the effects of the poloidal magnetic field. These two effects spread the radiation over a vertical height of the outer vessel wall of about 2m. This is confirmed by the measurements from the in-vessel cameras. The bremsstrahlung power in these detectors has been evaluated using the Heitler total cross-section and shows reasonable agreement with the measurements.

K-shell vacancy production. In many disruptions it has been observed by the radiation protected cameras that there are very weak X-ray signals between the onset of runaway generation and their eventual interaction with the wall. Contour plots show an clearly structured image (Fig. 2). Detailed examination of these images has led to the inescapable conclusion that they are direct images of the runaway beam. This is confirmed by the very clear correlation with the position signals from the magnetic measurements. It is believed that this image is formed by the runaways producing K-shell vacancies in metallic impurities in the residual plasma, resulting in K-line emission with energy $E_{Kz} = 5-8\text{keV}$. This radiation would not be confined to a narrow forward cone like the bremsstrahlung but would be emitted in all directions and detected with high efficiency. The radiated power, P_K , is correctly calculated if there is an influx of impurities at the time of disruption:

$$P_K = \sum n_r n_z \eta_z \sigma_z v_e E_{Kz} = j_r \sum n_z \eta_z \sigma_z E_{Kz} / e$$

where σ_z is the cross-section for K-shell vacancy production and is fairly independent of electron energy; η_z is the K-shell fluorescence yield and n_r is the density of runaways. The image offers the possibility of determining several new properties of the runaway beam, and the vertical height can be immediately determined as a function of time. The measurements show that the runaway beam starts in a small volume at the plasma



centre and grows in diameter as it moves towards the wall, but it never occupies more than a small fraction of the total volume. A delay between the negative voltage spike and the start of runaway generation is also seen and this may offer possibilities for mitigation of the adverse effects of the runaways. The delay may be caused either because the density is too high immediately following the disruption or because there is a high level of magnetic fluctuations which leads to the loss of electrons before they are able to be accelerated to high energies. The smoothness of the emission shows that the runaway beam is in a stable configuration until it hits the wall.

Safety factor (q) profile of runaways. In some discharges the runaway beam moves rapidly across a single line of sight which then gives the emission profile (Fig.3a). The observed signal is the line integral

$$S_K = \int j_r dl \Sigma n_z \eta_z \sigma_z E_{Kz} / e$$

which shows that these are a direct determination of the line integrated runaway current density (assuming σ_z

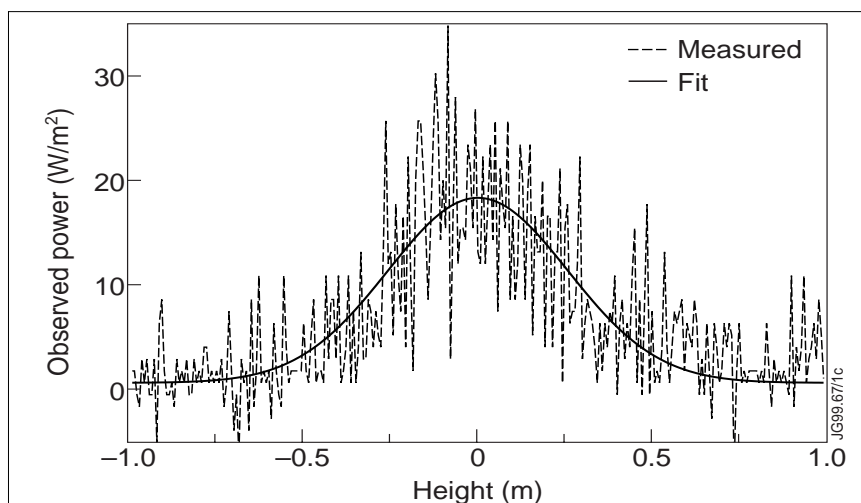


Fig. 3(a). Emission profile in a single X-ray channel as the runaway beam moves rapidly across its line of sight.

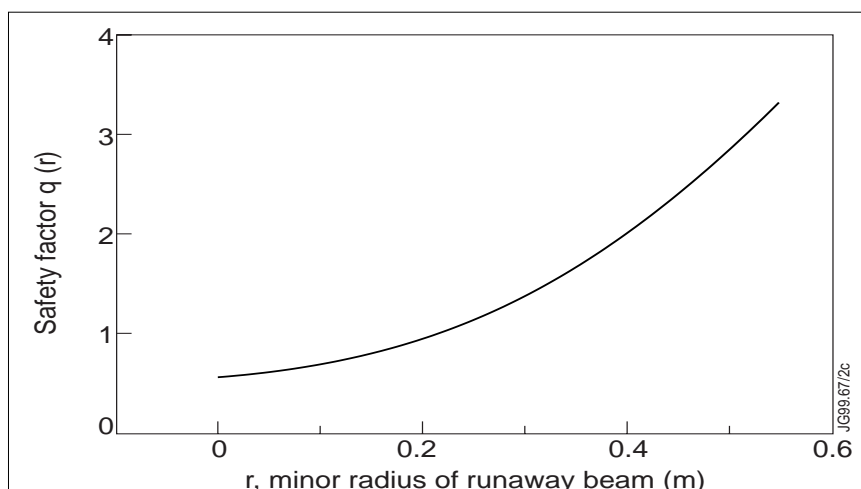


Fig. 3(b). Calculated q-profile from inversion of the line integrated X-ray data.

is independent of energy). The profile is gaussian. In Fig 3a the abscissa has been changed from time to vertical distance using the measured vertical velocity of the runaway beam. It is seen that the beam has a full width at half maximum of 0.37m. Inversion of this profile determines the localised emission which is proportional to the current density profile. Taking the total runaway current from the plateau value of the current trace allows the calculation of the q-profile. Figure 3b shows that q rises from about 0.5 at the centre to 3 at the edge of the runaway beam. This is similar to a normal tokamak discharge and may account for the stability of the

beam. It is also found that $q=3$ at the surface of the runaway beam as it begins to hit the wall. **Runaway-wall interactions.** The beam is basically stable until it hits the vessel wall except for some isolated hot spots that are sometimes seen which may be caused by ufo's which drift into the runaway beam. The interaction with the wall is seen to be over a very localised area

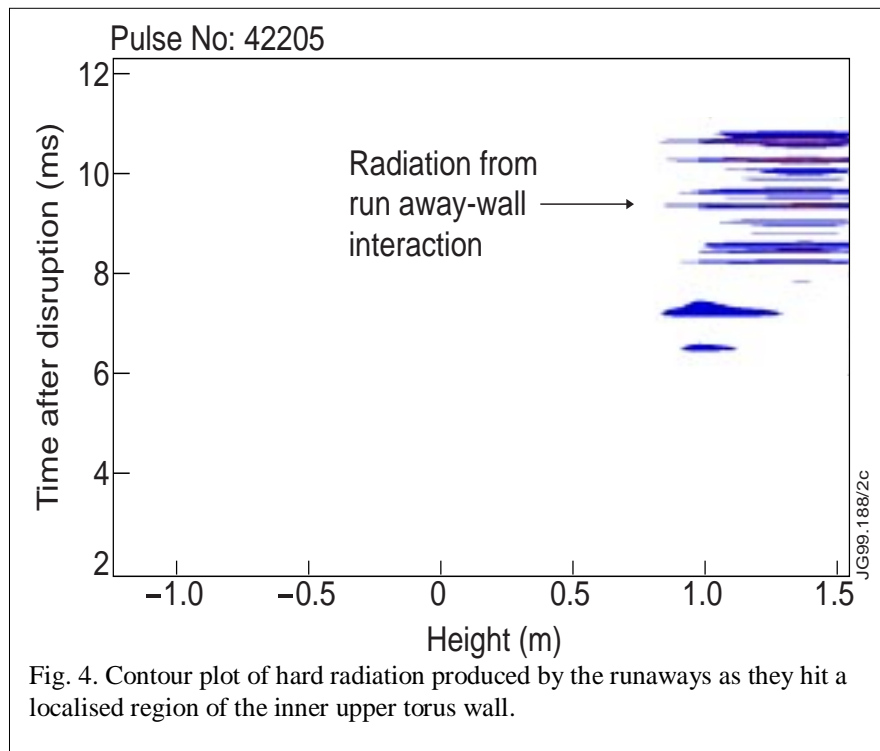


Fig. 4. Contour plot of hard radiation produced by the runaways as they hit a localised region of the inner upper torus wall.

with a poloidal dimension of less than 0.1m. The wall emission has a series of very rapid spikes contained within an overall time window of 2ms (Fig. 4.). In a disruption examined in detail, the K-shell emission intensity data determines that the diameter of the runaway beam at the moment of impact with the wall is 0.8m. The beam has a minor radial velocity of 190 m/s and all the runaways would therefore hit

the wall in 2.1ms, in good agreement with the measured value. It is therefore apparent that the runaway wall interaction is not caused by instabilities but is a simple consequence of the beam being driven into the wall at a uniform speed. The most probable explanation for the fast spikes is that the runaways have a very uneven spatial distribution on a series of concentric tori. This could be understood as a consequence of the extreme sensitivity of the production process to the ratio of the applied electric field to the Dreicer field. Minor variations of E/E_D on different flux surfaces would lead to huge variations in the number of runaways produced. In addition, if avalanche effects are important in the runaway generation process, it is possible that there are enhancements in the production rate on rational q -surfaces. Data from cameras on opposite sides of the torus show that the spikes are not toroidally symmetric, suggesting poloidal runaway current density variations on each flux surface. The runaway beam therefore appears to have a complex ribbon structure associated with the underlying poloidal field structure.

Conclusions. A detailed X-ray image of the runaway beam generated in a disruption has been observed. The image originates in line radiation following K-shell vacancy production by the runaways. From this the beam dimensions, its movement and stability have been determined. The localised nature of the interaction with the wall is also established and the rapid fluctuations in the runaway-wall interaction show that the beam is filamented. The current profile of the runaway beam and its q -profile has been determined.

- References** [1] Jaspers, R., Nuclear Fusion **36** (1996) 367.
[2] Gill, R.D., Nuclear Fusion **33** (1993) 1613.